A new type of half-quantum circulation in a macroscopic polariton spinor ring condensate

Gangqiang Liu[a], David W. Snoke[a,1], Andrew Daley[a,b], Loren N. Pfeiffer[c,1], and Ken West[c]

[a]Department of Physics and Astronomy, University of Pittsburgh, Pittsburgh, PA 15260; [b]Department of Physics and Scottish Universities Physics Alliance, University of Strathclyde, Glasgow G4 0NG, United Kingdom; and [c]Department of Electrical Engineering, Princeton University, Princeton, NJ 08544

Contributed by Loren N. Pfeiffer, January 13, 2015 (sent for review November 25, 2014; reviewed by Peter Littlewood)

We report the observation of coherent circulation in a macroscopic Bose–Einstein condensate of polaritons in a ring geometry. Because they are spinor condensates, half-quanta are allowed in where there is a phase rotation of π in connection with a polarization vector rotation of π around a closed path. This half-quantum behavior is clearly seen in the experimental observations of the polarization rotation around the ring. In our ring geometry, the half-quantum state that we see is one in which the handedness of the spin flips from one side of the ring to the other side in addition to the rotation of the linear polarization component; such a state is allowed in a ring geometry but will not occur in a simply connected geometry. This state is lower in energy than a half-quantum state with no change of the spin direction and corresponds to a superposition of two different elementary half-quantum states. The direction of circulation of the flow around the ring fluctuates randomly between clockwise and counterclockwise from one shot to the next; this fluctuation corresponds to spontaneous breaking of time-reversal symmetry in the system. This type of macroscopic polariton ring condensate allows for the possibility of direct control of the circulation to excite higher quantized states and the creation of Josephson junction tunneling barriers.

polariton condensates | ring condensates | quantized circulation | spinor condensates

Ring condensates, analogous to superconducting rings, have received much attention lately (1–9); among other predictions, a ring condensate allows the possibility of macroscopic superposition of states with different circulation. A ring condensate is topologically distinct from a condensate in a simply connected region.

With the advance of the field of polariton condensates in the past few years, it is a natural step to create a condensate ring in a microcavity polariton system. The polariton system allows direct, nondestructive observation of the momentum distribution, energy distribution, and spatial distribution of the particles as well as direct measurement of the coherence properties through interferometry. To make a macroscopic ring requires macroscopic transport distances as well as macroscopic coherence length. Macroscopic coherence has been achieved with polaritons with coherent motion over tens of micrometers with lifetimes of 10–20 ps (10, 11) and coherent motion over hundreds of micrometers with lifetimes of 150–200 ps (12–14). One advantage of the long-lifetime polariton systems is that the polaritons can move well away from the laser spot where they are generated, so that the laser can be viewed as a simple source term and does not interact with the condensate. General reviews of previous polariton work with shorter transport distances are in refs. 15–19.

The polaritons can be viewed as photons that have been given a small effective mass of the order of 10^{-4} times the mass of a vacuum electron and repulsive interactions, which are about 10^4 times stronger than the typical $\chi^{(3)}$ nonlinearities of photons in solids. The effective mass comes from the dispersion of the photons in a planar cavity, $\hbar\omega = \hbar c(k_\parallel^2 + k_\perp)^{1/2}$, where $k_\perp$ is fixed by the width of the cavity, which implies that $\hbar\omega \simeq E_0 + \hbar^2 k_\parallel^2 / 2m_{\rm eff}$ with $m_{\rm eff} = \hbar k_\perp / c$ for low $k_\parallel$. There are two circular polarization modes of the cavity photons corresponding to $m = \pm 1$ for the projection of the angular momentum on the z axis perpendicular to the plane. The strong interactions between photons are generated by mixing the photon states with a sharp excitonic resonance in a semiconductor inside the cavity, so that the photons pick up a fraction of the exciton–exciton interaction. Although their interactions are much stronger than the interactions of typical photons in a solid medium, the polaritons are still in the weakly interacting Bose gas regime.

The structure for these experiments is a planar cavity, in which the mirrors are distributed Bragg reflectors of AlAs/AlGaAs and the exciton medium consists of GaAs/AlGaAs quantum wells embedded in this cavity. This structure has the same design as that used in previous experiments, which allows coherent transport of polaritons over hundreds of micrometers in the 2D plane of the cavity (12–14). Recent measurements (14) give the cavity lifetime as 135 ps, which corresponds to a polariton lifetime of 200 ps or more. Although this lifetime may seem to be short compared with atoms evaporating from an optical trap on timescales of seconds, the polariton lifetime is sufficient for them to interact many times with each other. In these long-lifetime polariton systems, the ratio of lifetime in the trap to the particle–particle collision time can be of the order of 500:1, comparable with the ratio for cold atom condensates.

The lifetime of the polaritons and the strength of the interaction between the polaritons can be tuned by varying the energy difference between the photon states and the exciton states (known as the “detuning”), which leads to a varying degree of mixing of the photons and excitons. Because the planar cavity has a wedge that gives a gradient of cavity width, we can tune the strength of the polariton–polariton interactions simply by choosing different locations on the sample with different cavity width. There is a tradeoff in how much excitonic interaction

Significance

Polaritons are propagating states in certain solid-state systems that couple directly to light signals. This work gives a clear observation of quantized circulation of a polariton condensate in a ring; spontaneous quantized circulation is one of the key tests of true superfluidity. The quantized circulation seen here is a new type that is only possible in a spinor condensate in a ring geometry. Because polariton condensates can be made relatively easily in solid-state systems that can operate up to room temperature, the door is open to all kinds of superfluid effects of light in optical communications.

Author contributions: G.L. and D.W.S. designed research; G.L. performed research; L.N.P. and K.W. fabricated new semiconductor/optical structures; G.L., D.W.S., and A.D. analyzed data; and G.L. and D.W.S. wrote the paper.

Reviewers included: P.L., University of Chicago.

The authors declare no conflict of interest.

[1]To whom correspondence may be addressed. Email: snoke@pitt.edu or loren@princeton.edu.

This article contains supporting information online at www.pnas.org/lookup/suppl/doi:10.1073/pnas.1424549112/-/DCSupplemental.

character to give to the polaritons. Fewer interactions (more photon-like) allow long transport length, whereas more interactions allow better thermalization of the polariton gas through collisions and longer population lifetime.

Creating the Ring Condensate

For these experiments, we chose a region of the sample in which the polaritons were slightly more photon-like than exciton-like. We then created an in-plane harmonic potential using the inhomogeneous stress method that has previously been shown (20). Because a shift of the exciton energy also affects the exciton–photon detuning and therefore, the strength of the interaction between the polaritons, we must compensate for the effect of the stress on the detuning by our initial choice of the detuning at the location in the cavity. In the experiment reported here, the detuning at the location of interest was −6.7 meV without stress and +1.9 meV with the stress applied.

We then created a Gaussian potential energy peak inside this harmonic potential using a laser focused to a spot, which generates an exciton cloud. The laser was nonresonant, with photon energy 105 meV higher than the polariton energy. This optical pumping produced both excitons and polaritons at the laser focus spot. The excitons have a mass that is four orders of magnitude larger than that of the polaritons, and therefore, they diffuse, at most, about 10 μm from their point of creation; they therefore act as a quasistatic barrier for the polaritons (10–12). The sum of the harmonic potential and the Gaussian peak caused by the exciton cloud makes a Mexican hat potential. Fig. 1*A* shows our estimates for the different terms that contribute to the potential. Fig. 1*B* shows the intrinsic experimental energy profile recorded using a defocused laser, and Fig. 1*C* shows flow of the polaritons in the trap when the laser spot is focused not at the center of the trap but instead, on the right side. The polaritons clearly flow away from the laser spot, about 35 μm, to the minimum of the harmonic potential.

To create the ring trap, we moved the laser focus to near the center of the harmonic potential minimum, as shown in Fig. 1*A*. As in previous work (12), when the density of the central exciton peak exceeds a critical value, there is a sharp transition to occupation of the ground state of the trap. Fig. 2 shows the photon emission from the polaritons for two cases. Fig. 2*A* shows the emission from the laser focus when the density is below the critical density, and Fig. 2*B* shows the filling of the ring above the critical density threshold. As seen in Fig. 3*B*, which gives the energy spectrum for the same conditions as Fig. 2*B*, the condensate is monoenergetic, with a narrow line width limited by our spectral resolution of 0.08 meV. Although there are density variations around the ring, the condensate fills in low-potential areas to maintain a single energy. This ring condensate was observed under quasi-steady-state conditions, with a continuous flow of polaritons generated at the central laser spot and flowing into the ring to replace the loss of polaritons turning into external photons outside of the cavity while the laser is on for a duration of 25 μs. A period of 2.5 ms with the laser off between pulses was used to prevent heating of the sample.

The degree of spatial coherence of the condensate can be seen in an interference measurement. Fig. 4 *A*–*C* shows typical interference patterns when two copies of the spatial image of the condensate are overlapped with one of the images flipped: $x \to -x$. Fringes are seen across the entire image from one side to the other, showing that the coherence extends across the whole ring.

A close analysis shows that the number of fringes on the top of the interference patterns in Fig. 4 is not always equal to the number of fringes on the bottom. In other words, there is net circulation in the condensate, defined as $\Gamma = \oint \vec{v} \cdot d\vec{l}$, which implies that the phase cannot be continuous—in the ring geometry, the potential barrier at the center of the ring makes the density of the condensate zero where the discontinuity occurs.

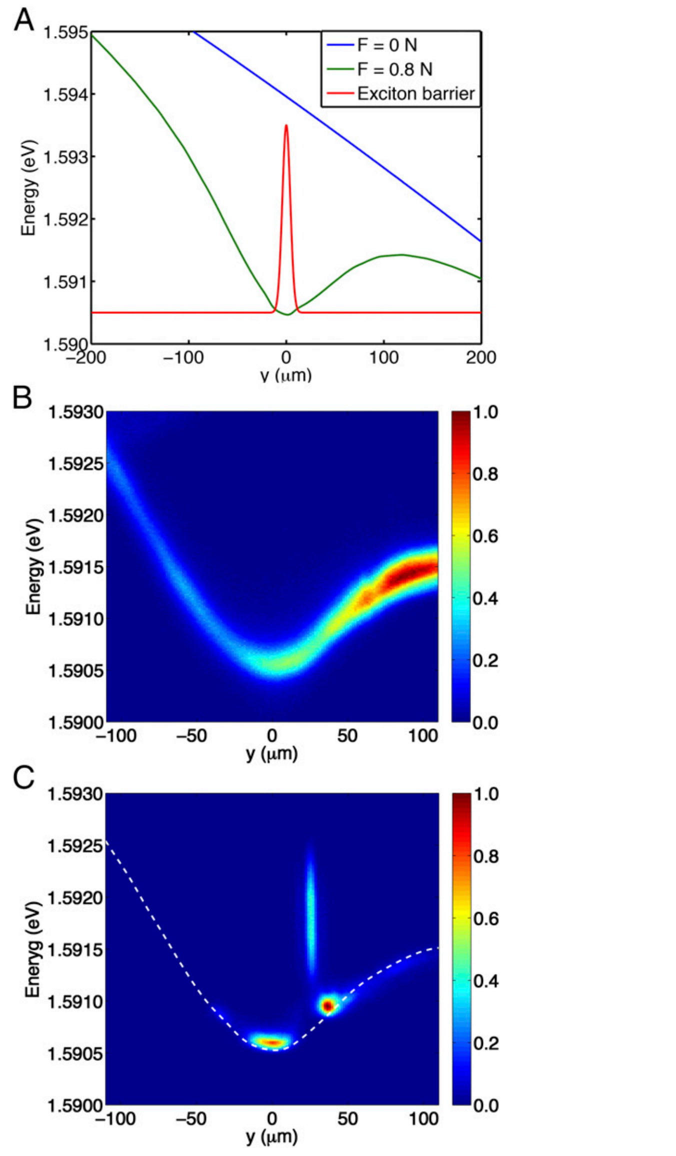

Fig. 1. (*A*) Plot of the three terms that contribute to the potential energy felt by the polaritons when they are condensed. The blue line is the energy gradient caused by the wedge in the cavity width (applied force on the stressor $F = 0$). The green line is the energy shifted by applied stress to have a harmonic potential minimum (applied force on the stressor $F = 0.8$ N. The red line is the potential peak created by a nearly static cloud of excitons. (*B*) The harmonic trap and gradient potentials seen in the photon emission spectrum from the polaritons at very low density generated using a defocused laser. (All color bars are normalized to maximum intensity $= 1.0$.) (*C*) The same system when the laser spot is tightly focused and set to one side instead of at the center of the trap. The vertical line is emission from polaritons at the laser spot shifted up in energy by repulsion from the static exciton cloud. Polaritons flow to both sides of this spot, including to the global minimum.

The circulation can be seen in the phase maps that are produced from the interferometric data shown in Fig. 4 *D*–*F*.

The interference patterns are stable over the duration of the 25-μs pulses used here. The pattern fluctuates from one pulse to the next, split with equal probability between a pattern with clockwise or counterclockwise circulation about 90% of the time and about 10% of the time showing an equal number of fringes on the top and bottom. We never see a difference of more than one fringe.

For the interference geometry that we use here, a phase change of 2π around the ring in the phase map corresponds to

PHYSICS

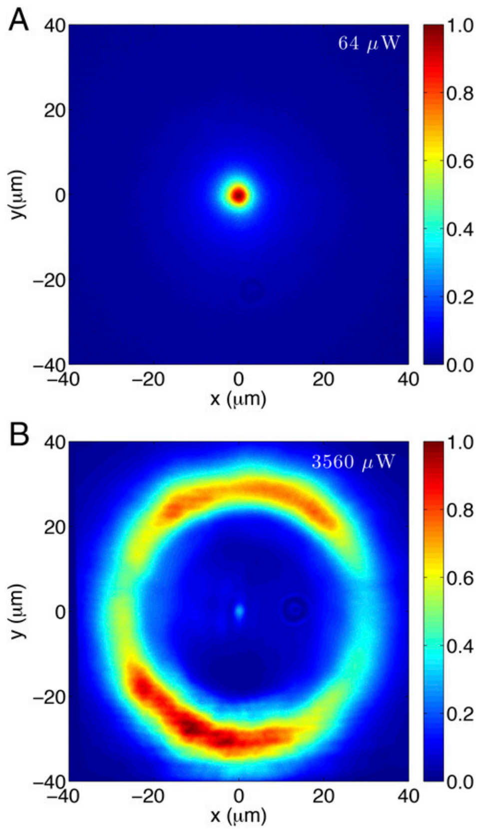

Fig. 2. (*A*) Real-space image below critical threshold (64 μW average laser power for a 1% duty cycle with 25-μs duration pulses). (*B*) Real-space image for the same conditions as *A* but above critical threshold for condensation (3.56 mW average laser power). The light polarizations are summed in these images.

a total phase change of only π around the ring, because the interference pattern gives the phase change of the condensate relative to itself in opposite directions (*SI Text*). These phase maps, therefore, indicate that the spinor nature of the polaritons with two degenerate states is important, because a scalar condensate must have a phase change of $2\pi n$ around a closed path.

Determining the Circulation State

Fig. 5*A* shows the direction of linear polarization at various points on the ring deduced from measurements of the full Stokes vector of the light emitted at different points around the ring (raw images of the Stokes vector data are in *SI Text*). As seen in Fig. 5*A*, the linear polarization angle rotates by 180°, whereas the circular component flips handedness on opposite sides of the ring. This polarization pattern is striking given that the underlying exciton states in GaAs-based structures have a fourfold symmetry, which is seen in a fourfold rotational symmetry of the polarization pattern under incoherent conditions (21, 22), and the eigenstates of the polariton states are linearly polarized (22). The orientation of the pattern is not connected to the underlying crystal symmetry; instead, it is fixed relative to the gradient of potential that exists in the system, which comes from the wedge in the cavity width. The polarization pattern of the condensate also does not depend on the polarization of the laser that generates the polaritons at the central spot.

The interference pattern and the polarization measurements can both be understood as the effects of quantized angular momentum in a spinor condensate. The generic effect of half-quantization has been worked out for spinor atom condensates (23), *d*-wave superconductors (24) and in particular, by Rubo (25), the case of polaritons in a simply connected geometry; half-quantized vortices were reported experimentally for a polariton condensate localized in a submicrometer disorder minimum (26, 27). However, the state that we see here is distinct from the half-vortex state by Rubo (25) and is favored only in a ring geometry.

The Rubo state, when generalized to a ring geometry, consists of a π-rotation in phase around a closed path accompanied by a π-rotation of the polarization angle around the same path. In terms of the linear polarization components in the plane of the sample, the azimuthal angle dependence of the Rubo state around a circle of constant radius can be written as (25)

$$\vec{\varphi}_{k,m}(\theta) = \sqrt{n(\theta)}e^{im\theta}\left[f\begin{pmatrix}\cos(k\theta)\\ \sin(k\theta)\end{pmatrix} - i\,\mathrm{sgn}(km)\sqrt{1-f^2}\begin{pmatrix}\sin(k\theta)\\ -\cos(k\theta)\end{pmatrix}\right]. \quad [1]$$

Here, $m,k\in\{-1/2,+1/2\}$ selects the rotation directions for the phase and the polarization, respectively; $n(\theta)$ is the effective 1D density of the condensate, f is a real constant that gives the degree of circular polarization, and $|f|$ must be less than 1. In the Rubo vortex state, f can depend on the radius r, whereas in a ring, we can approximate that f is nearly constant. For each combination of k and m, this ansatz gives a degree of circular polarization $c=\mathrm{sgn}(km)2f\sqrt{1-f^2}$ that does not depend on θ and a linear polarization angle that rotates as $k\theta$. In the absence of interactions and in a homogeneous ring $n(\theta)=n$, these states with $|f|=1/\sqrt{2}$ are eigenstates of the Hamiltonian that consist of the kinetic energy

$$H_{\mathrm{kin}} = -\frac{\hbar^2}{2m}\nabla^2 \equiv -\frac{\hbar^2}{2mR^2}\frac{d^2}{d\theta^2}, \quad [2]$$

where m is the effective mass of the polaritons.

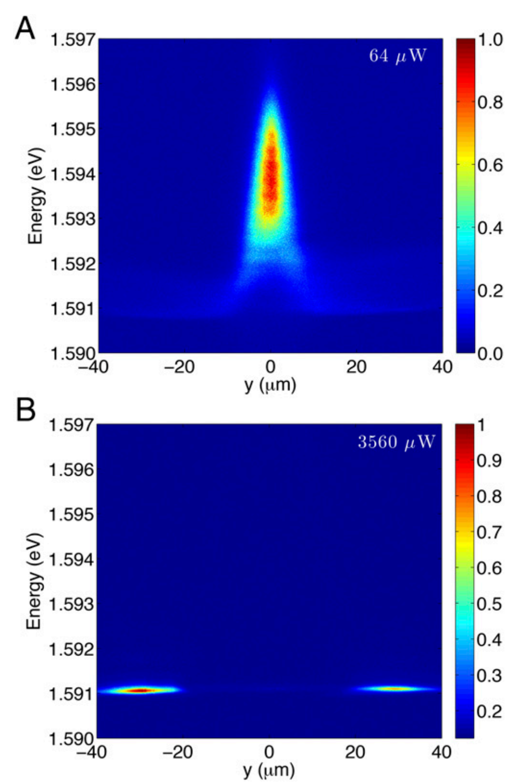

Fig. 3. Spectral images along y for $x=0$ for the same data as shown in Fig. 2. (*A*) Spectral image for $x=0$ for the conditions in Fig. 2*A*. (*B*) Spectral image for $x=0$ for the same conditions as in Fig. 2*B*.

In a simply connected geometry, only half-quanta of the type given by Eq. **1** are allowed, because there is an implicit boundary condition that the polarization must be continuous at $r=0$. However, in a ring geometry, this condition is relaxed, and other wave functions with half-quanta of circulation also satisfy the boundary condition that the wave function be single-valued. The polarization pattern that we observe is reproduced by using the following form for the wave function, which is the same except for a single sign change:

$$\vec{\psi}_{k,m}(\theta)=\sqrt{n(\theta)}e^{im\theta}\left[f\begin{pmatrix}\cos(k\theta)\\ \sin(k\theta)\end{pmatrix} + i\,\mathrm{sgn}(km)\sqrt{1-f^2}\begin{pmatrix}\sin(k\theta)\\ \cos(k\theta)\end{pmatrix}\right]. \qquad [3]$$

This equation gives the polarization map shown in Fig. 5*B* for the choice $f=-0.3$. Like the Rubo state, it provides a half-quantum of circulation with a phase rotation direction chosen by the sign of m, but it involves a flip of the circular polarization around the ring. For these states, the degree of circular polarization is given by $c=-\mathrm{sgn}(km)2f\sqrt{1-f^2}\cos(2k\theta)$, so that the circular polarization direction (i.e., the z component of the particles with $J=1$) flips from one side of the ring to the other as seen in the experimental data in Fig. 5*A*. The linear polarization angle is given by

$$\frac{1}{2}\arg\left(\frac{f+\mathrm{sgn}(km)\sqrt{1-f^2}\,e^{2ik\theta}}{f\,e^{2ik\theta}-\mathrm{sgn}(km)\sqrt{1-f^2}}\right), \qquad [4]$$

which can rotate in either direction, and this direction is determined by the sign of k in the ansatz. Note that any sign of k and m can be paired here. As discussed in *SI Text*, this ansatz also reproduces the interference patterns that we observe.

The state seen here is not an eigenstate of kinetic energy. As discussed further in *SI Text*, the ansatz (Eq. **3**) that fits our experimental data corresponds to the superposition

$$\vec{\psi}_{k,m}=-\sqrt{2}\left(0.95\vec{\varphi}^{0}_{\frac{1}{2},\frac{1}{2}}+0.3\vec{\varphi}^{0}_{\frac{1}{2},-\frac{1}{2}}\right), \qquad [5]$$

where $\varphi^0_{k,m}$ indicates the Rubo states (Eq. **1**) with $f=0$, which are chosen because they give us an orthogonal basis of states with well-defined physical properties. In other words, the observed state is a superposition of different half-quantized circulating states. Although a superposition of different angular–momentum states may seem odd, there is no in-principle reason for the system to favor a pure angular momentum state over the observed spin-flipping circulating state. Both states satisfy the boundary conditions. The state given by Eq. **3** is not allowed in a simply connected geometry, however, because the kinetic energy would diverge at $r=0$.

The fact that the stable state seen here is not an energy eigenstate is likely related to both the effect of particle–particle

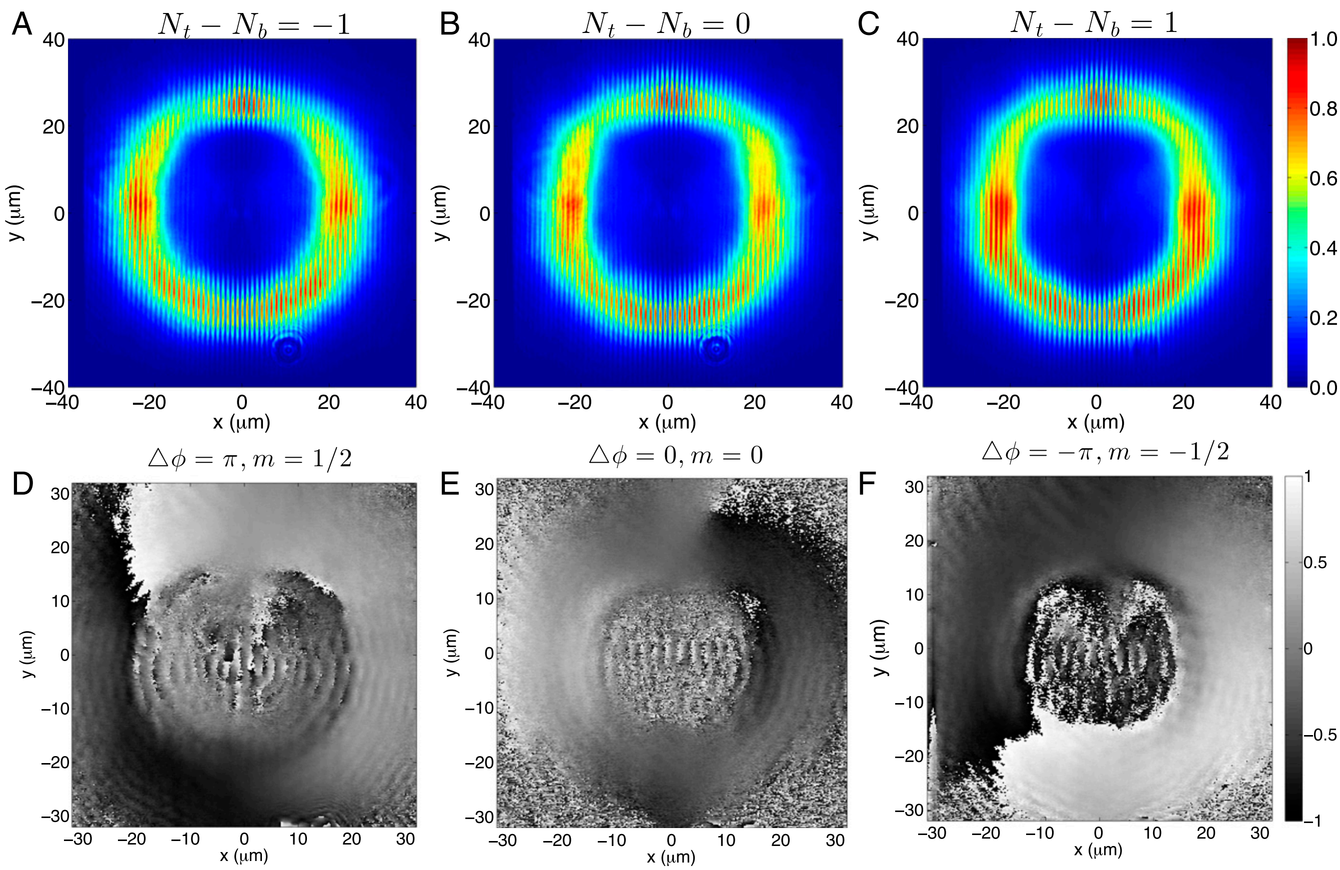

Fig. 4. (*A*) Interference pattern between two images of the condensate with one flipped across the y axis for average excitation laser power of 3.56 mW in single shots with 25-μs duration. There is one more fringe on the bottom (N_b) than on the top (N_t) of the ring. (*B*) Pattern for another single shot under the same conditions with an equal number of fringes on the top and bottom of the ring. (*C*) Pattern for another single shot with one more fringe on the top. (*D*) The phase map extracted from the interference pattern shown in *A*. The circulation is counterclockwise. (*E*) Phase map for the interference pattern of *B* showing no net circulation. (*F*) Phase map for *C* showing clockwise circulation. The $\Delta\phi$ labels above *D*–*F* indicate the net phase shift around the ring. Because the interference pattern measures the phase shift of the ring condensate relative to itself in the opposite direction, the net phase shift around the ring is one-half of that shown in the phase map.

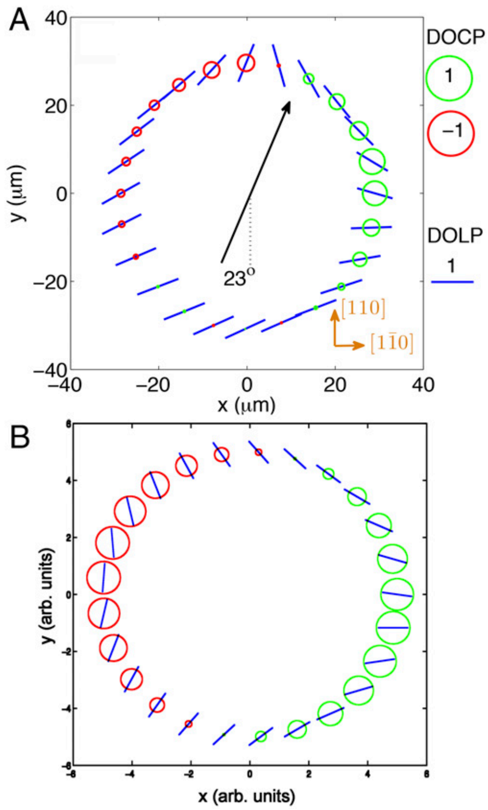

Fig. 5. (*A*) Experimental results for the polarization of the light emission from the ring at various positions. The lengths of the solid blue lines are proportional to the degrees of linear polarization (DOLP), and the radii of the circles are proportional to the degrees of circular polarization (DOCP) (green, right-handed; red, left-handed). The arrow shows the direction of downhill flow of the polaritons in the gradient of the cavity. (*B*) Theoretical polarization pattern for the condensate wave function given in Eq. **3** with $k = m = -1/2$ and $f = -0.3$.

interactions and the dynamic quasisteady-state conditions of generating the ring. We discuss the modifications that come from taking into account polariton–polariton interactions in *SI Text*.

Discussion and Future Directions

The stability of the polarization pattern observed in these experiments seems to be caused by symmetry breaking related to the optical spin–Hall effect for polaritons (28). This effect comes about because of the energy difference of the transverse electric and transverse magnetic modes of the photons in the cavity at finite in-plane momentum. Polaritons moving under the force of the cavity gradient will preferentially have linear polarization orthogonal to their direction of motion. When these polaritons scatter elastically into other k states with the same energy, they will scatter into a superposition of polarizations in the new direction, which will precess, giving a circular polarization component. As shown in ref. 28, the handedness of this circular polarization will be opposite for opposite directions of scattering. Although the optical spin-Hall effect may be small, it gives a symmetry-breaking term that corresponds to the circular polarization components being different on opposite sides of the downhill gradient, which we observe in these experiments. Below the condensate threshold, there is no significant circular polarization component of the photoluminescence from the ring. Above the condensation threshold, the high occupation of the condensate amplifies scattering processes, so that any small symmetry breaking term can lead to the condensate adopting a new symmetry.

Because the condensate must satisfy the boundary conditions of the ring, it cannot have the underlying fourfold rotational symmetry of the GaAs crystal unless it is in a much higher angular momentum state. The spin-flipping state with half-quantum of circulation that we see is actually well-matched to the real-space separation of the different circular handedness favored by the optical spin–Hall effect in the presence of the cavity gradient. The polarization rotation is, therefore, not a spontaneously broken symmetry. However, because the same polarization pattern can satisfy the boundary conditions of the ring with either handedness $m = \pm 1/2$ of the flow (phase gradient) around the ring, we see that the direction of the circulation does change randomly, because this degree of freedom has spontaneously broken symmetry. Future theoretical work will address the dynamical considerations of how the ring condensate forms and how it gains a circulation direction. Under some circumstances, a noncirculating state can be unstable when generation and decay are accounted for, such as, for example, the vortex that appears in a bathtub drain (29).

Recent work with a laser-generated ring trap (30) showed a superposition (i.e., a standing wave or two counterrotating polariton waves in high-momentum states). The main difference between that experiment and the work presented here is that the lifetime of the polaritons in our work is about an order of magnitude larger than in the work in ref. 30. The longer lifetime allows the polaritons in this work to cool down and thermalize to the bottom of the trap (as seen in Fig. 3), which allows the condensate to be in the true ground state of the ring. In the work in ref. 30, the polaritons maintained the energy that they had when they were generated by the laser. The momentum of the polaritons seen in ref. 30 was, therefore, fixed by that initial energy. There was no evidence of spontaneous symmetry breaking of the circulation direction under those conditions.

Additional experimental work in our ring traps can use a resonant laser beam to inject angular momentum onto the condensate (that is, to stir it). It is not clear whether injecting new particles with finite momentum will simply raise the amplitude of the condensate in its existing half-quantum state or if the condensate will prefer to jump to a higher angular momentum state. Both are ways in which the condensate can increase its total momentum. We also have the possibility of introducing small barriers in the ring using a laser-generated exciton cloud to create Josephson junctions analogous to those used in a ring superconducting quantum interference device (SQUID). Because we can observe the interference patterns directly from the light leaking through the mirrors, we can nondestructively measure the phase map for all of the states that we produce.

As we have seen, the polarization rotation is pinned in this system, whereas the direction of circulation of current around the ring is not. The laser focused at the center of the ring does not introduce any circulation. As a result, we see a random occurrence of circulation to the left or right, even as the polarization is pinned. These experimental results can, therefore, be seen as an example of spontaneous time-reversal symmetry breaking leading to a persistent current around the ring with a phase coherence time at least 100,000 times longer than the lifetime of any one particle in the condensate.

Because we have a macroscopic ring geometry that is topologically distinct from a simply connected geometry, a different topology of the circulation is allowed, with the spin of the particles flipping around the ring even as the particles remain in a single macroscopic wave function. The spin-flipping state with quantized flow cannot be continuously transformed into a state with a full quantum of circulation or a state with a half-quantum of circulation and no spin flip. The quantized angular momentum state seen here is different from the typical case of pairs of vortices of opposite vorticity generated because of turbulence (31, 32) and also, can be produced on demand as opposed to needing to search for a pinned vortex at a random location in a disordered landscape, which was the case for the work in ref. 26.

ACKNOWLEDGMENTS. This work has been supported by National Science Foundation Grants DMR-1104383 and PHY-1148957. The work at Princeton University was partially funded by the Gordon and Betty Moore Foundation as well as the National Science Foundation Materials Research Science and Engineering Center Program through Princeton Center for Complex Materials Grant DMR-0819860.

1. Ryu C, Blackburn PW, Blinova AA, Boshier MG (2013) Experimental realization of Josephson junctions for an atom SQUID. *Phys Rev Lett* 111(20):205301.
2. Ryu C, et al. (2007) Observation of persistent flow of a Bose-Einstein condensate in a toroidal trap. *Phys Rev Lett* 99(26):260401.
3. Andersen MF, et al. (2006) Quantized rotation of atoms from photons with orbital angular momentum. *Phys Rev Lett* 97(17):170406.
4. Ramanathan A, et al. (2011) Superflow in a toroidal Bose-Einstein condensate: An atom circuit with a tunable weak link. *Phys Rev Lett* 106(13):130401.
5. Wright KC, Blakestad RB, Lobb CJ, Phillips WD, Campbell GK (2013) Driving phase slips in a superfluid atom circuit with a rotating weak link. *Phys Rev Lett* 110(2):025302.
6. Beattie S, Moulder S, Fletcher RJ, Hadzibabic Z (2013) Persistent currents in spinor condensates. *Phys Rev Lett* 110(2):025301.
7. Hallwood DW, Burnett K, Dunningham J (2006) Macroscopic superpositions of superfluid flows. *New J Phys* 8:180.
8. Hallwood DW, Brand J (2011) Engineering mesoscopic superpositions of superfluid flow. *Phys Rev A* 84(4):043620.
9. Kanamoto R, et al. (2011) Quantum superpositions of flow states on a ring. *J Opt* 13(6):064011.
10. Wertz E, et al. (2011) Spontaneous formation and optical manipulation of extended polariton condensates. *Nat Phys* 6(11):860.
11. Cristofolini P, et al. (2013) Optical superfluid phase transitions and trapping of polariton condensates. *Phys Rev Lett* 110(18):186403.
12. Nelsen B, et al. (2013) Dissipationless flow and sharp threshold of a polariton condensate with long lifetime. *Phys Rev X* 3(4):041015.
13. Steger M, et al. (2013) Long range ballistic motion and coherent flow of long lifetime polaritons. *Phys Rev B Condens Matter Mater Phys* 88(23):235314.
14. Steger M, Gautham C, Snoke DW, Pfeiffer L, West K (2014) Slow reflection and two-photon generation of microcavity exciton-polaritons. *Optica* 2(1):1.
15. Kavokin A, Baumberg JJ, Malpuech G, Laussy FP (2011) *Microcavities* (Oxford Univ Press, London).
16. Snoke DW (2012) *Exciton-Polaritons in Microcavities (Springer Series in Solid State Sciences 172)*, eds Timofeev V, Sanvitto D (Springer, Berlin).
17. Deng H, Haug H, Yamamoto Y (2010) Exciton-polariton Bose-Einstein condensation. *Rev Mod Phys* 82(2):1489.
18. Carusotto I, Ciuti C (2012) Quantum fluids of light. *Rev Mod Phys* 85(1):299.
19. Snoke D, Littlewood P (2010) Polariton condensates. *Phys Today* 63:42.
20. Balili R, Snoke DW, Pfeiffer L, West K (2006) Actively tuned and spatially trapped polaritons. *Appl Phys Lett* 88(3):031110.
21. Sinclair NW, et al. (2011) Strain-induced darkening of trapped excitons in coupled quantum wells at low temperature. *Phys Rev B Condens Matter Mater Phys* 83(24): 245304.
22. Balili R, et al. (2010) Huge splitting of polariton states in microcavities under stress. *Phys Rev B Condens Matter Mater Phys* 81(12):125311.
23. Sinha S, Nath R, Santos L (2011) Trapped two-dimensional condensates with synthetic spin-orbit coupling. *Phys Rev Lett* 107(27):270401.
24. Machida M, Koyama T, Kato M, Ishida T (2004) Electronic structure of a half vortex. *Physica C Supercond* 412(pt 1):367.
25. Rubo YG (2007) Half vortices in exciton polariton condensates. *Phys Rev Lett* 99(10):106401.
26. Lagoudakis KG, et al. (2009) Observation of half-quantum vortices in an exciton-polariton condensate. *Science* 326(5955):974–976.
27. Manni F, Léger Y, Rubo YG, André R, Deveaud B (2013) Hyperbolic spin vortices and textures in exciton-polariton condensates. *Nat Commun* 4:2590.
28. Kavokin A, Malpuech G, Glazov M (2005) Optical spin hall effect. *Phys Rev Lett* 95(13):136601.
29. Keeling J, Berloff NG (2008) Spontaneous rotating vortex lattices in a pumped decaying condensate. *Phys Rev Lett* 100(25):250401.
30. Dreismann A, et al. (2014) Coupled counterrotating polariton condensates in optically defined annular potentials. *Proc Natl Acad Sci USA* 111(24):8770–8775.
31. Manni F, et al. (2013) Spontaneous self-ordered states of vortex-antivortex pairs in a polarization condensate. *Phys Rev B Condens Matter Mater Phys* 88(20):201303.
32. Tosi G, et al. (2011) Onset and dynamics of vortex-antivortex pairs in polariton optical parametric oscillator superfluids. *Phys Rev Lett* 107(3):036401.